Grazing incidence reflectivity and total electron yield effects in soft x-ray absorption spectroscopy

Alders, D.; Hibma, T.; Sawatzky, G. A.; Cheung, K. C.; van Dorssen, G. E.; Roper, M. D.; Padmore, H. A.; van der Laan, G.; Vogel, J.; Sacchi, M.

Published in:
Journal of Applied Physics

DOI:
10.1063/1.366153

Grazing incidence reflectivity and total electron yield effects in soft x-ray absorption spectroscopy

D. Alders, T. Hibma, G. A. Sawatzky, K. C. Cheung, G. E. van Dorssen, M. D. Roper, H. A. Padmore, G. van der Laan, J. Vogel, and M. Sacchi

Citation: Journal of Applied Physics **82**, 3120 (1997); doi: 10.1063/1.366153
View online: https://doi.org/10.1063/1.366153
View Table of Contents: http://aip.scitation.org/toc/jap/82/6
Published by the American Institute of Physics

Grazing incidence reflectivity and total electron yield effects in soft x-ray absorption spectroscopy

D. Alders, T. Hibma, and G. A. Sawatzky
Materials Science Center, University of Groningen, 9747 AG Groningen, The Netherlands

K. C. Cheung, G. E. van Dorssen, M. D. Roper, H. A. Padmore, and G. van der Laan[a)]
Daresbury Laboratory, Warrington WA4 4AD, United Kingdom

J. Vogel and M. Sacchi
Laboratoire pour l'Utilisation du Rayonnement Electromagnetique, Université Paris-Sud, F-91405 Orsay, France

(Received 18 March 1997; accepted for publication 16 June 1997)

We report on a study of grazing incidence absorption and reflection spectra of NiO in the region of the Ni $2p$ edge. The aim is to evaluate the distortion of the near edge spectrum by the critical angle behavior of individual components within the spectrum. This can be used to improve the separation of multiplets and enhance low spectral weight line shapes like charge transfer satellites. The measured spectra have been compared with calculations using an optical model. © *1997 American Institute of Physics.* [S0021-8979(97)05618-1]

I. INTRODUCTION

Core level spectroscopies such as magnetic x-ray dichroism (MXD) and x-ray resonant magnetic scattering are tools to study the magnetic properties of ferro-, ferri- and antiferromagnetic systems.[1,2] These techniques can provide detailed magnetic information, such as the separate orbital and spin magnetic moments.[3,4] Recently, dichroic interference effects were reported by Kao *et al.*[5] using circularly polarized soft-x-ray reflectivity. The authors observed a strong angle dependence of the circular dichroism, whereby the asymmetry ratio defined between the reflected right and left circularly polarized light exceeds, for certain angles, the degree of circular polarization of the incident light. It is generally known that in (angle dependent) XAS measurements, deviations from the true absorption line shape occur, depending for example on the detection technique used.[6–8] For instance, in the case of total electron yield one is restricted by the relation between the escape depth of electrons and the absorption cross section of a particular transition,[9] which is referred to as saturation. Several other independent mechanisms can also be responsible for a strong distortion of absorption line shapes. In some cases it is even hard to detect the real absorption structure in the normal incidence spectrum, as is the case for most of the dipole allowed $3d \rightarrow 4f$ transitions in rare earth compounds.[10]

One can perceive these deviations from the true absorption line shapes as an artifact of XAS in general, but one can also try to use the underlying mechanisms to obtain the nondistorted line shape. Van der Laan and Thole[6] demonstrated this for LaF_3 by analyzing the total electron yield as a function of angle of incidence. Abbate *et al.*[11,12] used the saturation effect to study the mean probing depth of total electron yield quantitatively. In this article we present experimental results that are dominated by strong interference effects at grazing incidence using linear polarized light, which can provide information about the underlying multiplet structure in the absorption spectrum. In order to discriminate between near edge distortions and MXD effects, the direction of the electric vector was kept constant by using s-polarized light. Our method can be used to deform the line shape of absorption edges in a controlled way. The experimentally observed deformation of line shapes at grazing incidence can be successfully explained by a classical optical model that includes the polarization of the incident light. This has been demonstrated by André *et al.*[13] in studies of specular reflectivity at glancing angles at the Si $1s$ edge of SiO_2. This edge shows quite well resolved structures over an energy range of 15 eV above the edge. In the more recent x-ray absorption studies of $3d$ transition metal $2p$ edges and rare earth $3d$ edges the white line shapes are dominated by atomiclike multiplet structure coming from a large number, 50 or more, of closely spaced states with strongly differing intensities so that in the normal experiment the weaker structures are unresolved. This unresolved structure contains, never the less, important information concerning the details of the ground state electronic structure and orbital and spin moments. As we will show a detailed investigation of the grazing incidence angle dependent absorption and reflection makes these weak *hidden* transitions visible although a detailed *optical* analysis is required to extract information on the peaks positions and oscillator strengths.

II. EXPERIMENTAL DETAILS

A 27 monolayer NiO sample was epitaxially grown, in a layer by layer fashion, on the (100) surface of a MgO single crystal.[14] The measurements were done at the Synchrotron Radiation Source at Daresbury Laboratory using the undulator beam line 5U.1. The source and optical system have been described in detail elsewhere,[15] but briefly consist of a 1-m-long, 10-period undulator, followed by an entrance slitless, variable included angle, plane grating monochromator, operating from 65 to 1000 eV. The vertical aperture into the monochromator was restricted to give a highly polarized

a)Electronic mail: g.vanderlaan@dl.ac.uk

 0021-8979/97/82(6)/3120/5/$10.00

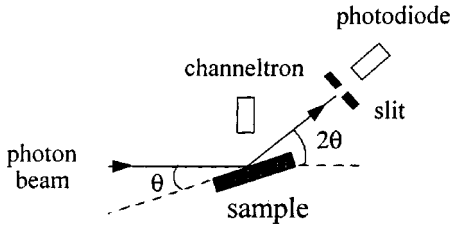

FIG. 1. The experimental geometry for the simultaneous absorption and reflection measurements.

photon beam, the calculated linear polarization being larger than 90% with the electric vector in the orbit plane of the electron beam. A purpose built, high vacuum, computer controlled reflectometer was used to perform the measurements.

The geometry of the experimental arrangement is shown in Fig. 1. The sample deflects the beam vertically and the rotation axis is horizontal, i.e., perpendicular to the plane of the paper in Fig. 1. The electric vector of the light is thus parallel to the rotation axis. The photon beam was collected to give a horizontal width of 2 min and vertical height of 0.2 min at the sample. The reflected beam from the sample was detected using an entrance-slitted GaAsP/Au photodiode with a vertical slit height of 0.1 mm and a horizontal length of 10 mm. Total electron yield was simultaneously recorded using a high current channeltron situated vertically and directly above the sample. A grid over the front of the channeltron was biased at $+200$ V to ensure good collection efficiency of all electrons. The rotary motions for the sample and photodiode were independent and were produced by high precision rotary tables with 0.001° resolution. The angular positions of the sample and photodiode tables were controlled via stepping motors under computer control. The control software allowed scanning of the detector angle at fixed sample angle, or scanning of sample and detector angle in a $\theta-2\theta$ arrangement. For a given θ and 2θ of interest, the photon energy was scanned to record the reflectivity (photodiode) and electron yield (channeltron) spectra.

III. RESULTS

In Fig. 2 we show the experimental dependence on the angle θ between the (100) plane and the propagation direction of the light, of the Ni $L_{2,3}$ absorption edges of NiO (100). Note that the angle between the electric vector **E** and the (100) plane is kept constant, since **E** is perpendicular to the plane of incidence as defined in Fig. 1. The origin of the peak structures in the x-ray absorption spectrum has been explained in Ref. 16. One can clearly see that at low glancing angles, below $\theta=5°$, the electron yield spectrum becomes highly distorted. The most intense feature in the L_3 region becomes suppressed due to the influence of saturation i.e., all peaks tend to have comparable heights at grazing angles. In the pre-edge a dip evolves that is preceded by a bump at even lower angles, with its maximum shifting towards higher energy for decreasing angle of incidence. Furthermore, one can observe the critical angle behavior for all individual multiplet lines in the spectrum and as a result the normally eclipsed multiplet structures become resolved. The best separation between the multiplet components on the high energy side of the NiL_3 edge is observed at $\theta=1.55°$. Note that the spectral features in the NiL_3 edge are fixed in energy, while the first peak in the NiL_2 edge shifts towards lower energy. One should also note that the charge transfer satellite $2p^5 3d^{10}\underline{L}$ (where $\underline{L}$ denotes a ligand hole) at 860 eV, becomes prominent at this angle.

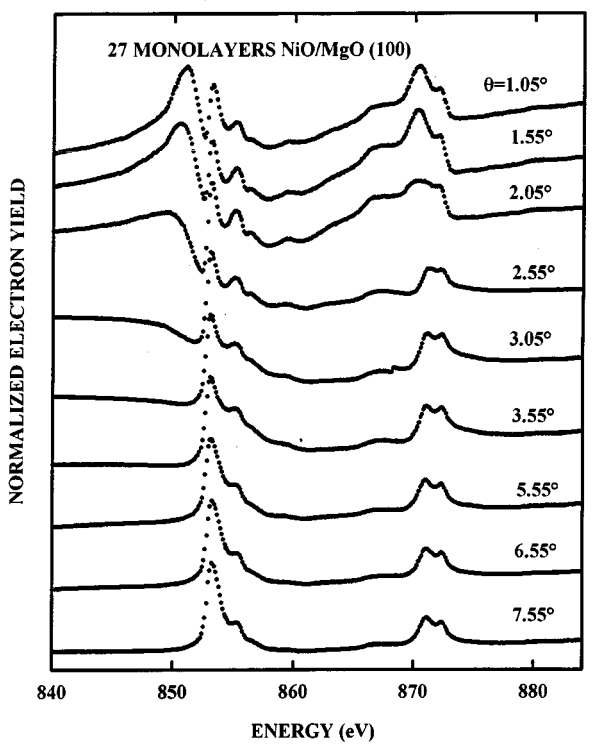

FIG. 2. Measured glancing angle (θ) dependence of the electron yield at the Ni $L_{2,3}$ absorption edges of epitaxially grown NiO on MgO (100) single crystal using s-polarized light.

In Fig. 3 we compare the low glancing angle spectrum at $\theta=1.55°$ with a high glancing angle spectrum at θ

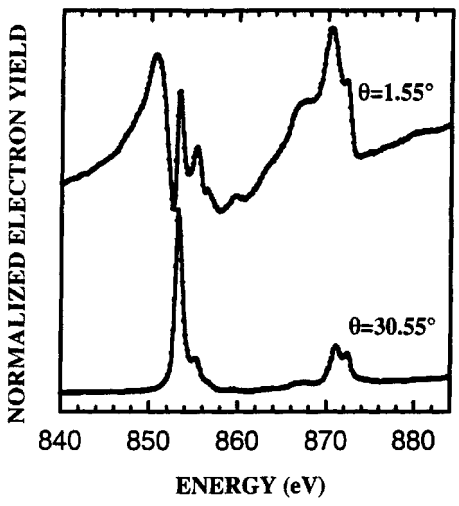

FIG. 3. Measured electron yield spectra obtained at $\theta=30.55°$ and $\theta=1.55°$ demonstrating the improved energy resolution of the multiplet line shapes.

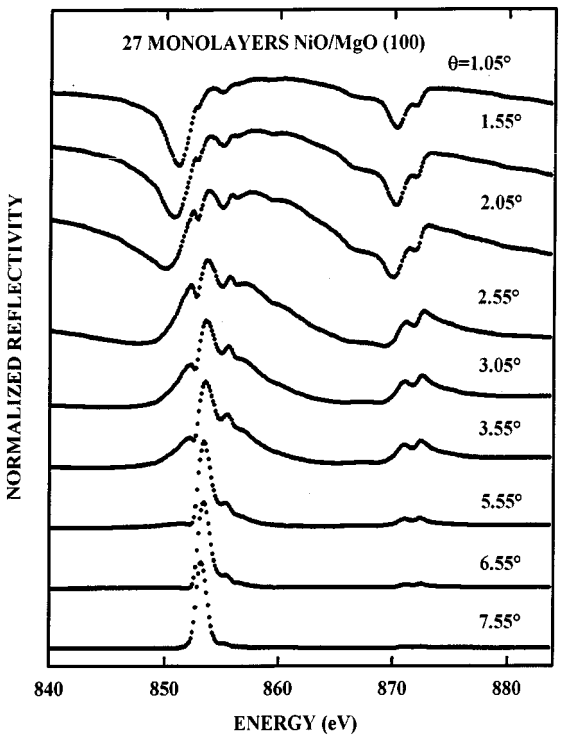

FIG. 4. Measured glancing angle (θ) dependence of the reflectivity while scanning through the Ni $L_{2,3}$ absorption edges using s-polarized light.

$=30.55°$. One can clearly see that the multiplet components at the high energy side of the NiL_3 edge show enhanced features at low glancing angles.

In Fig. 4 we show the measured dependence of the reflectivity on the grazing angle θ in the region of the Ni$L_{2,3}$ absorption edges using s-polarized light. The reflectivity spectra were obtained simultaneously with the total electron yield of Fig. 2, as explained in Sec. II. At the highest glancing angles ($\theta>6°$), the reflectance spectrum essentially consists only of the single most intense feature in the electron yield L_3 spectrum. Below $\theta=5.55°$ a peak in the pre-edge of the L_3 evolves. At lower glancing angles ($\theta<5.55°$), the reflection spectrum starts to resemble the high angle electron yield spectrum.

IV. DISCUSSION

The physical origin for the improved separation of the multiplet structure in the electron yield at grazing angles is the real part of the dielectric function, which convolutes the spectrum in a rather complicated way. Suppose there are two transitions possible with equal transition probability, which are close in energy. Scanning through the multiplet structure of an absorption edge means that a peak is deformed by the real part of the absorption line shape of another peak at lower energy. This can also be observed in the experimental spectra where the first peak of the NiL_2 edge is shifting to lower energies while the position of the peaks in the NiL_3 edge remains almost unchanged. The general outcome is that in the region between the two transitions the spectral weight intensity will be lowered. The modified spectrum obtained seems to have ''increased structure.'' Unfortunately, the interference is not as transparent as stated here and is most prominent at glancing incidence as can be appreciated from the Fresnel equations. In order to predict the angle dependence over a large energy range one should know all the matrix elements responsible for the background and all the line shape broadening mechanisms must also be taken into account. In the most simple cases, the lifetime broadening can be simulated by a Lorentzian line shape, while the instrumental broadening due to the response function of the x-ray monochromator and beamline optics can be represented by a Gaussian line shape. Other mechanisms such as autionization can result in more complex Fano-like line shapes,[17] which require an additional parameter for the asymmetry.

In the example of the Ni$L_{2,3}$ edges in NiO, the wavelength of the x rays used ($\sim$14.5Å) is much larger than the atomic spacing, so diffraction effects are not expected. In our evaluation here we neglect these effects and use an optical model to explain the data. We also neglect interference effects within the sample due to the finite layer thickness.

The probability that an electron excited at depth z will reach the detector is denoted by $Ce^{-z/L}$. The factor C takes into account the detector efficiency, the escape depth L is independent of z but depends weakly on the energy of the electron and the different decay channels of the core hole created. The parameters L and C are assumed to be independent on the direction of the electric field. The attenuation of the absorption is described by the decrease in intensity I with depth

$$I=I_0e^{-\alpha z}, \tag{1}$$

where α is the absorption coefficient given by

$$\alpha=\frac{2\omega n_i}{c}, \tag{2}$$

where n_i is the imaginary part of the complex refractive index ($\tilde{n}=n_r+in_i$), which is related to the real part n_r, by a Kramers–Kronig transformation and c is the velocity of light. The dielectric function and the complex refractive index are related by

$$\tilde{n}^2=\tilde{\epsilon}'+i\epsilon''. \tag{3}$$

The quantum yield per incident photon is then given by integration to infinity[6]

$$Y=C(1-R)\alpha\int_0^\infty dz\ e^{-\alpha z}e^{-z/L}=C(1-R)\ \frac{\alpha L}{\alpha L+\sin\ \theta}, \tag{4}$$

where R is the reflectivity in the case of s-polarized light given by the Fresnel equation

$$R=\left|\frac{\cos\ \theta-\sqrt{\tilde{n}^2-\sin^2\ \theta}}{\cos\ \theta+\sqrt{\tilde{n}^2-\sin^2\ \theta}}\right|^2. \tag{5}$$

The complex dielectric function derived for the case that electrons are bound by elastic forces given by Hooke's law can be found in textbooks as[18]

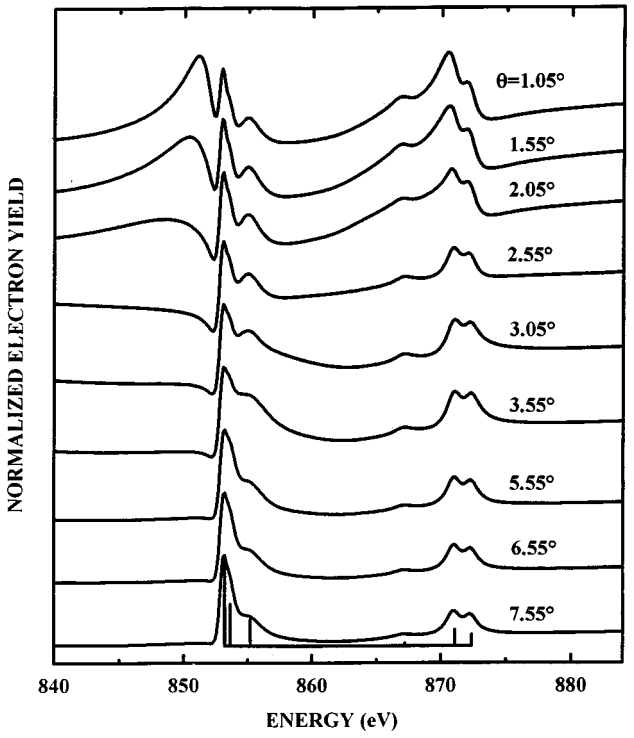

FIG. 5. Theoretical glancing angle (θ) dependence of the Ni $L_{2,3}$ absorption edges using Eq. (4) and the Lorentzian lines indicated by the sticks under the bottom spectrum.

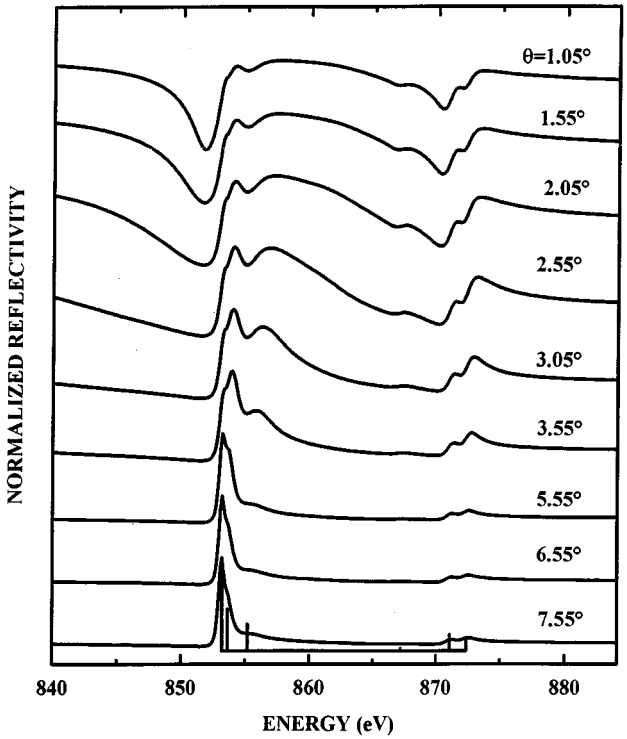

FIG. 6. Theoretical glancing angle (θ) dependence of the reflectivity while scanning through the Ni $L_{2,3}$ absorption edges using Eq. (4) and the Lorentzian lines indicated by the sticks under the bottom spectrum.

$$\tilde{\epsilon}=\tilde{\epsilon}_{\text{back}}+\frac{Ne^2}{m\epsilon_0}\sum_j \frac{f_j}{\omega_j^2-\omega^2-i\gamma_j\omega}, \tag{6}$$

where f_j is the oscillator strength of the jth resonance at frequency ω_j, N is the number of dipoles per unit volume, and $\tilde{\epsilon}_{\text{back}}$ is the complex dielectric function taking into account also absorption edges at lower energies.

In Fig. 5 we show a comparison of the best theoretical fit of Eq. (4) to the angular dependent electron yield data. The theoretical fit was obtained by the Levenberg–Marquardt algorithm,[19] using nine Lorentzian oscillators, the background dielectric function is $\tilde{\epsilon}_{\text{back}}=0.9979+i1.316\times10^{-3}$ and the escape depth of the electrons was set to 50 Å.[16] The overall agreement with experiment, as shown in Fig. 5, is very good. Only small peaks such as the charge-transfer satellites could not be fitted due to the limited number of oscillators used. Note that the full multiplet of the $2p^53d^9$ final state is given by $6\times10=60$ possible final states plus continuum states such as $4s$ states. Simulations including Fano line shapes did not significantly improve the fitting. This suggests that the coupling of the final state multiplet with the continuum states can in first order be treated by Lorentzian line shape broadening. Unfortunately, the set of fitting parameters, which is used to explain all angles, was not unique, i.e., slightly different parameters gave an almost equally good fitting. Nevertheless, the physics behind the changes in the spectrum has been explained. Note that in principle a fit including a Fano line shape could give detailed information about the autoionization process and the oscillator strength of the continuum.[10]

In Fig. 6 we show the theoretical reflectivity spectra as obtained from fitting of the electron yield spectra. A comparison with Fig. 4 shows that the agreement between theory and experiment is very good. Only the pre-edge peak in the experimental spectra at 852 eV, which evolves below $\theta=5.55°$, cannot be explained.

In Fig. 7 we show the real and imaginary part of the complex refractive index as obtained from the optical model. The latter shows the true undistorted absorption spectrum. In Fig. 8 we demonstrate the influence of the critical angle behavior of reflections off the surface for different multiplet lines. We therefore focus on the Ni L_3 edge and plot the

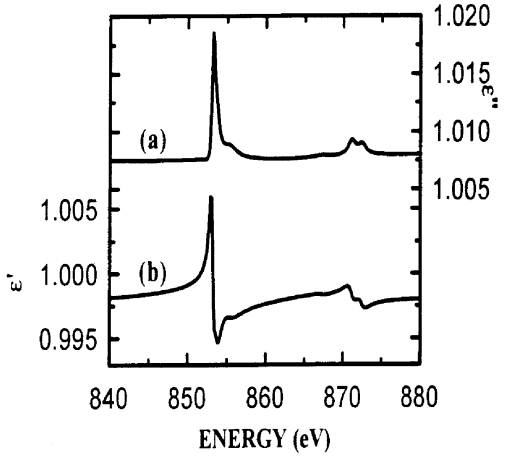

FIG. 7. (a) The imaginary and (b) real part of the dielectric function as obtained using the optical model.

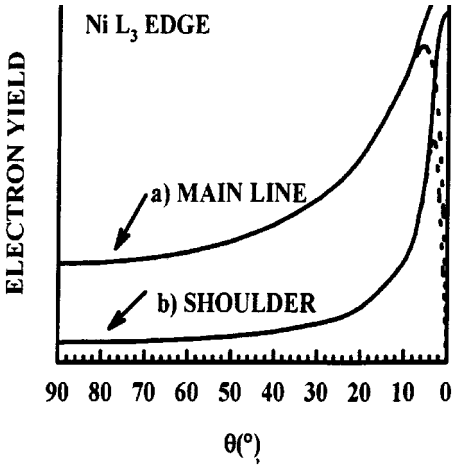

FIG. 8. The influence of saturation and reflectivity in the (a) main line and (b) shoulder of Ni L_3 edge of NiO as calculated with the optical model. The solid line is without correcting for the reflectivity and the dashed line is the calculated absorption including reflectivity.

electron yield for the maximum of the white line and its shoulder at the high energy side, with (dotted line) and without (full line) the factor of Eq. (6), as a function of angle θ. In Fig. 8 we can see that at lower glancing angles the electron yield increases for both the white line and the shoulder. This means that at lower glancing angles more electrons are able to escape from the sample. However, the change in yield as a function of angle is different for both multiplets, already referred to as saturation. Taking into account reflections off the sample surface will effect the electron yield as indicated (dotted lines) below a certain angle. For the white line (shoulder) of the Ni L_3 edge deviations from the curve without reflections start at 9° (5°). This clearly shows the influence of the line strength on the critical angle.

V. CONCLUSIONS

We performed grazing incidence absorption and reflection experiments in the soft x-ray region. With a simple optical model based on the Fresnel equations we were able to explain the dramatic change in absorption spectra and revealed the physical origin of this phenomenon. This model has the potential to explain the white line energy shift observed in some cases for the polarization dependent Cu $2p$ absorption spectra in $(Bi_{0.84}Pb_{0.16})_2Sr_2CaCu_2O_8$ as a function of angle of incidence.[20] Small changes in the dielectric function over the absorption edge can have dramatic effects on x-ray absorption spectra at grazing incidence. These experiments provide more detailed information about the underlying multiplet structure of white lines. The complex critical angle behavior of the multiplet line shapes can also be exploited to study low intensity satellite structures. One could in principle obtain information about the configuration interaction with the continuum states by exploiting the Fano line shapes.

ACKNOWLEDGMENT

The authors would like to acknowledge B. T. Thole for fruitful discussions.

[1] B. T. Thole, G. van der Laan, and G. A. Sawatzky, Phys. Rev. Lett. **55**, 2086 (1985).
[2] J. P. Hannon, G. T. Trammell, M. Blume, and D. Gibbs, Phys. Rev. Lett. **61**, 1245 (1988); **62**, 2644 (1989).
[3] B. T. Thole, P. Carra, F. Sette, and G. van der Laan, Phys. Rev. Lett. **68**, 1943 (1992).
[4] P. Carra, B. T. Thole, M. Altarelli, and X. Wang, Phys. Rev. Lett. **70**, 694 (1993).
[5] C. C. Kao, C. T. Chen, E. D. Johnson, J. B. Hastings, H. J. Lin, G. H. Ho, G. Meigs, J. M. Brot, S. L. Hulbert, Y. U. Idzerda, and C. Vettier, Phys. Rev. B **50**, 9599 (1994).
[6] G. van der Laan and B. T. Thole, J. Electron Spectrosc. Relat. Phenom. **46**, 123 (1988).
[7] Y. U. Idzerda, C. T. Chen, H-J. Lin, C. Meigs, G. H. Ho, and C. C. Kao, Nucl. Instrum. Methods Phys. Res. A **347**, 134 (1994).
[8] F. M. F. de Groot, M. A. Arrio, Ph. Sainctavit, Ch. Cartier, and C. T. Chen, Solid State Commun. **92**, 991 (1994).
[9] W. Gudat and C. Kunz, Phys. Rev. Lett. **29**, 169 (1972).
[10] B. T. Thole, G. van der Laan, J. C. Fuggle, G. A. Sawatzky, R. C. Karnatak, and J. M. Esteva, Phys. Rev. B **32**, 5107 (1985).
[11] M. Abbate, J. B. Goedkoop, F. M. F. de Groot, M. Grioni, J. C. Fuggle, S. Hoffman, H. Petersen, and M. Sacchi, Surf. Interface Anal. **18**, 65 (1992).
[12] J. Vogel and M. Sacchi, Phys. Rev. B **49**, 3230 (1994); J. Electron Spectrosc. Relat. Phenom. **67**, 181 (1994).
[13] J. M. André, A. Maquet, and R. Barchewitz, Phys. Rev. B **25**, 5671 (1982).
[14] S. D. Peacor and T. Hibma, Surf. Sci. **301**, 11 (1994).
[15] C. S. Mythen, G. van der Laan, and H. A. Padmore, Rev. Sci. Instrum. **63**, 1313 (1992).
[16] G. van der Laan, J. Zaanen, G. A. Sawatzky, R. C. Karnatak, and J. M. Esteva, Phys. Rev. B **33**, 4253 (1986).
[17] U. Fano, Phys. Rev. **124**, 1866 (1961).
[18] M. Born and E. Wolf, *Principles of Optics* (Pergamon, New York, 1975).
[19] D. Marquardt, SIAM J. Appl. Math. **11**, 431 (1963).
[20] M. Abbate, M. Sacchi, J. J. Wnuk, L. W. M. Schreurs, Y. S. Wang, R. Lof, and J. C. Fuggle, Phys. Rev. B **42**, 7914 (1990).